Please cite this article in press as: Hayashi et al., Reconstitution of the Mouse Germ Cell Specification Pathway in Culture by Pluripotent Stem Cells, Cell (2011), doi:10.1016/j.cell.2011.06.052

Cell

Reconstitution of the Mouse Germ Cell Specification Pathway in Culture by Pluripotent Stem Cells

Katsuhiko Hayashi,[1,3] Hiroshi Ohta,[1,3] Kazuki Kurimoto,[1,3] Shinya Aramaki,[1] and Mitinori Saitou[1,2,3,*]
[1]Department of Anatomy and Cell Biology, Graduate School of Medicine
[2]Institute for Integrated Cell-Material Sciences
Kyoto University, Yoshida-Konoe-cho, Sakyo-ku, Kyoto 606-8501, Japan
[3]JST, CREST, Yoshida-Konoe-cho, Sakyo-ku, Kyoto 606-8501, Japan
*Correspondence: saitou@anat2.med.kyoto-u.ac.jp
DOI 10.1016/j.cell.2011.06.052

SUMMARY

The generation of properly functioning gametes in vitro requires reconstitution of the multistepped pathway of germ cell development. We demonstrate here the generation of primordial germ cell-like cells (PGCLCs) in mice with robust capacity for spermatogenesis. PGCLCs were generated from embryonic stem cells (ESCs) and induced pluripotent stem cells (iPSCs) through epiblast-like cells (EpiLCs), a cellular state highly similar to pregastrulating epiblasts but distinct from epiblast stem cells (EpiSCs). Reflecting epiblast development, EpiLC induction from ESCs/iPSCs is a progressive process, and EpiLCs highly competent for the PGC fate are a transient entity. The global transcription profiles, epigenetic reprogramming, and cellular dynamics during PGCLC induction from EpiLCs meticulously capture those associated with PGC specification from the epiblasts. Furthermore, we identify Integrin-β3 and SSEA1 as markers that allow the isolation of PGCLCs with spermatogenic capacity from tumorigenic undifferentiated cells. Our findings provide a paradigm for the first step of in vitro gametogenesis.

INTRODUCTION

The germ cell lineage ensures the creation of new individuals in most multicellular organisms, perpetuating the genetic and epigenetic information across the generations. Accordingly, in vitro reconstitution of germ cell development is one of the most fundamental challenges in biology. In mice, germ cell fate is induced in the epiblasts at around embryonic day (E) 6.0 by the bone morphogenetic protein 4 (Bmp4) signaling from the extraembryonic ectoderm (Lawson et al., 1999). The primordial germ cells (PGCs), the origins for both the oocytes and the spermatozoa, are established at around E7.25 as a small cluster of alkaline phosphatase (AP)-positive cells in the extraembryonic mesoderm (Ginsburg et al., 1990; Saitou et al., 2002). Blimp1 (Prdm1) and Prdm14 are critical transcriptional regulators for the PGC fate (Kurimoto et al., 2008; Ohinata et al., 2005; Vincent et al., 2005; Yamaji et al., 2008). Essentially all of the epiblast cells from E5.5∼E6.0 are competent to express *Blimp1* and *Prdm14* in response to Bmp4, and the PGC-like cells induced from the epiblasts ex vivo can form functional sperm when transplanted into neonatal testes lacking endogenous germ cells (Ohinata et al., 2009). A robust induction of germ cell fate in vitro might therefore be possible if one could generate the pregastrulating (E5.5∼6.0) epiblast-like cells in vitro.

Two groups of pluripotent cells in mice, the inner cell mass (ICM) of preimplantation blastocysts at E3.5–E4.5 and the epiblast of postimplantation embryos at E5.5–E6.5, give rise to two distinct pluripotent stem cell (PSC) types in vitro, which are called embryonic stem cells (ESCs) and epiblast stem cells (EpiSCs), respectively (Brons et al., 2007; Evans and Kaufman, 1981; Tesar et al., 2007). ESCs bear the ground state (naive) pluripotency and can contribute to all lineages when introduced into blastocysts, whereas EpiSCs exhibit a primed pluripotency and are unable to contribute to chimeras when injected into blastocysts (Nichols and Smith, 2009). These two cell types show distinct morphologies, cytokine dependence, gene expression, and epigenetic profiles. Notably, human (h) ESCs are more like mouse (m) EpiSCs, reflecting the difficulty of capturing the naive pluripotency in nonrodent species (Nichols and Smith, 2009).

There have been attempts to generate gametes or PGCs in vitro from ESCs both in mice and humans (for review, see Daley, 2007; Saitou and Yamaji, 2010). These attempts were based on a strategy of isolating cells that express a germ cell marker(s) in embryoid bodies differentiated spontaneously under undefined conditions. Consequently, these efforts were inefficient at obtaining the cells of interest (less than ∼1.0%) and were unsuitable for analyzing the events that take place before the emergence of germ cell-like cells. Critically, the induced cells have never been demonstrated to contribute to healthy offspring. There was a single report claiming the generation of live yet abnormal offspring from gamete-like cells derived from ESCs (Nayernia et al., 2006), but whether these offspring carry a full haploid contribution from ESC-derived cells remains to be determined (Daley, 2007).

On the other hand, EpiSCs retain attributes of the original epiblasts and are a potential source for the generation of germ cell-like cells in vitro (Hayashi and Surani, 2009; Tesar et al.,

2007). A subpopulation of the EpiSCs express *Blimp1* under a self-renewing condition, and a minority of them are positive for stella (Pgc7/Dppa3), a marker for the established PGCs. However, the emergence of these cells from the EpiSCs occurs at a low frequency even in the presence of BMP4 (~1.5%), and the function of these cells in vivo has not been demonstrated (Hayashi and Surani, 2009). The relatively inefficient induction of the PGC fate from EpiSCs may reflect the fact that the EpiSCs acquire properties that are incompatible for efficient PGC induction during their culture. Note that the competence of the epiblast to form PGCs diminishes markedly after ~E6.25 (Ohinata et al., 2009).

Given these findings, we explored a condition under which ESCs and induced PSCs (iPSCs) (Takahashi and Yamanaka, 2006) with naive pluripotency are induced into pregastrulating epiblast-like cells from which, in turn, PGC-like cells are induced. We demonstrate here the establishment of a defined culture system reconstituting the PGC specification pathway in mice.

RESULTS

Pregastrulating Epiblast-like Cells from ESCs

We initially explored a variety of conditions to induce the PGC fate from the EpiSC aggregates or from EpiSCs cultured in two dimensions, but we did not find conditions that improved on those described previously (Figure S1 available online and data not shown) (Hayashi and Surani, 2009). We therefore decided to explore a distinct strategy for the induction of the PGC fate from PSCs, based on the following considerations: (1) ESCs cultured under a serum- and feeder-free condition with a MAPK inhibitor (PD0325901), a GSK3 inhibitor (CHIR99021), and leukemia inhibitory factor (LIF) (2i+LIF) exhibit a uniform property similar to the ICM/preimplantation epiblast (~E4.5) state (the ground state) (Nichols et al., 2009; Ying et al., 2008); (2) ESCs form PGCs within a few days when introduced into the blastocysts; and (3) in the continuous presence of Activin A (ActA) and basic fibroblast growth factor (bFGF), ESCs convert into EpiSC-like cells exhibiting similarities to the postimplantation (~E6.5) epiblasts (Guo et al., 2009; Han et al., 2010). We reasoned that the ground state ESCs might rapidly differentiate into pregastrulating epiblast-like cells with high competence for the PGC fate under conditions similar to those used to induce EpiSC-like cells.

We derived ESCs from the E3.5 blastocysts bearing *Blimp1-mVenus* and stella-*ECFP* (BVSC) transgenes (Ohinata et al., 2008) under the ground state condition. Among a variety of conditions examined, stimulation with ActA, bFGF, and knockout serum replacement (KSR) at a concentration as low as 1% resulted in the uniform induction of ESCs into flattened epithelial structures resembling the epiblasts over the 3 day period (Figures 1A and 1B). Stimulation with higher concentrations of KSR (2%–20%) resulted in the maintenance of a dome-shaped ESC morphology: the higher the KSR concentration, the greater the maintenance of the ESC-like state. In contrast, stimulation with ActA and bFGF without KSR resulted in an increased rate of cell death (data not shown).

Upon stimulation with ActA, bFGF, and 1% KSR, the cells grew rapidly for the first 2 days but thereafter underwent a significant extent of cell death, and the number of the surviving cells at day 3 was similar to that at day 2 (Figure 1D). As in ESCs, we observed no BVSC expression in the induced epiblast-like cells (hereafter called EpiLCs) during the 3 day differentiation period (Figure 1B). An independent ESC line bearing *Prdm14*-mVenus (P14V) transgenes (Yamaji et al., 2008) exhibited a similar differentiation upon the same stimulation: P14V was expressed in the ESCs but declined along with the EpiLC induction (Figure 1B). Immunofluorescence (IF) analysis showed that, during the EpiLC induction, Oct3/4 (Pou5f1) was continuously expressed, but Sox2 and Nanog were decreased by day 2 and day 1, respectively (Figure 1C). The downregulation of Nanog during EpiLC differentiation was in sharp contrast to its continued expression in EpiSCs (Figure S1C) (Hayashi and Surani, 2009).

We quantified the expression of key genes in the EpiLCs, EpiSCs, and E5.75 epiblasts by quantitative (Q)-PCR (Figure 1E). During EpiLC differentiation, *Oct3/4* was expressed at a constant level, whereas genes more tightly associated with the ICM state, such as *Sox2*, *Nanog*, and *Prdm14*, as well as *Zfp42* (*Rex1*), *Tbx3*, *Tcl1*, *Esrrb*, *Klf2*, *Klf4*, and *Klf5*, were downregulated to levels similar to those in the epiblasts. In EpiSCs, *Sox2*, *Nanog*, and *Klf5* were retained at levels similar to those in ESCs. In both EpiLCs and EpiSCs, *Wnt3*, *Fgf5*, and *Dnmt3b*, which are upregulated in the epiblasts, were indeed elevated. Notably, in EpiLCs, as in the epiblasts but in contrast to EpiSCs, endoderm markers such as *Gata4*, *Gata6*, and *Sox17* were downregulated or remained at very low levels. *Blimp1*, which, apart from PGCs, shows expression in the visceral and definitive endoderm, was downregulated in EpiLCs, but not in EpiSCs (Figure 1E and Figures S1B and S1C). These findings indicate that EpiLCs show properties that are consistent with pregastrulating epiblasts, whereas EpiSCs bear distinct characteristics.

PGC-like Cell Induction from EpiLCs

We next examined whether the EpiLCs would be induced into PGC-like cells under conditions that fostered induction of the epiblast cells to the PGC fate (a floating condition in GMEM with 15% KSR [GK15] with cytokines including BMP4) (Ohinata et al., 2009). We first induced the ESCs and day (d) 1/2/3 EpiLCs (~1000 cells) for 2 days and evaluated their BVSC expression. No strong BV induction was observed in any of the aggregates cultured in the GK15 alone or the GK15 with LIF (Figure 2A and Figure S2A). In contrast, when cultured with BMP4 or BMP4 and LIF, robust BV induction (~40%) (BV-positive [+], strongly positive for BV as defined by fluorescence activated cell sorting [FACS]) was observed in the aggregates of d2 and d3 EpiLCs, but not ESCs or d1 EpiLCs (Figure 2A and Figure S2A). We noted that aggregates from d3 EpiLCs were much smaller and looked less integrated compared to those from other origins (Figure 2A). SC was not observed in any of the cultures during the 2 day period (Figure 2A and Figure S2A). Thus, d2 EpiLCs are highly competent to express *Blimp1* in response to BMP4 and for subsequent healthy growth.

We next examined whether d2 EpiLCs form BVSC(+) PGC-like cells when cultured for a longer period. When these cells were cultured in the GK15 alone, no significant BVSC induction was observed during the 6 day period (Figure 2B and Figure S2B). When they were cultured with BMP4, BV was strongly induced on day 2 (~35.3%). On day 4, the aggregates grew well and

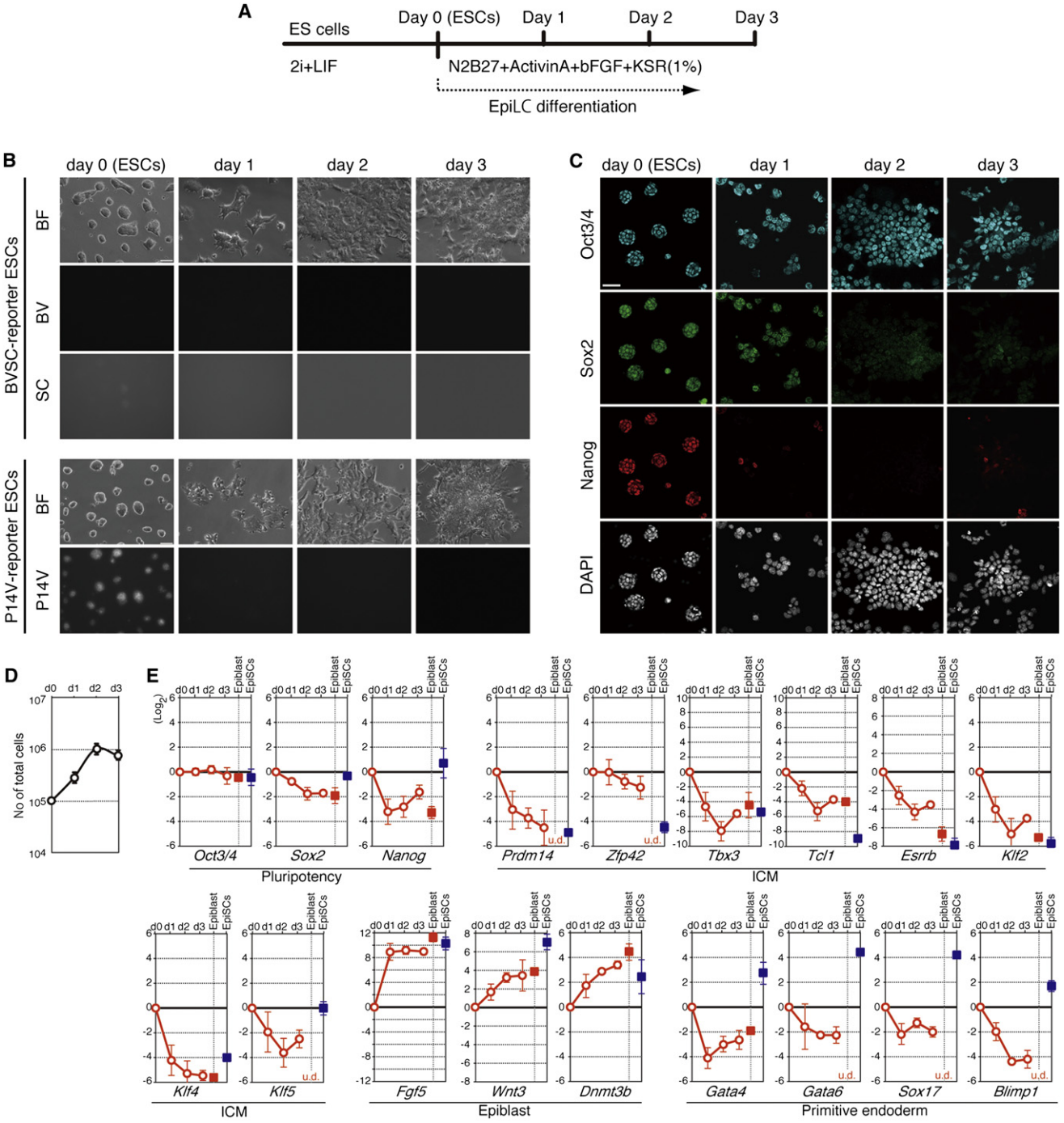

Figure 1. Epiblast-like Cell Induction from ESCs

(A) The scheme for epiblast-like cell (EpiLC) induction.

(B) EpiLC induction from BVSC (top) and P14V (bottom) ESCs. Bright-field and fluorescence images from the reporters are shown. Scale bar, 50 μm.

(C) Immunofluorescence (IF) analysis of Oct3/4 (top row), Sox2 (second), and Nanog (third) expression counterstained by DAPI (bottom) during the EpiLC (day [d] 1, d2, and d3) induction. Scale bar, 50 μm.

(D) Cell growth during the EpiLC induction. Average cell numbers with standard deviations (SDs) from three independent experiments are shown.

(E) Gene expression profiles during the EpiLC induction, of the epiblasts at E5.75, and of the EpiSCs as measured by Q-PCR. For each gene examined, the ΔCT from the average CT values of the two independent housekeeping genes *Arbp* and *Ppia* was calculated. The value for ESCs was set as 0. For each point, the average value from three, two, and two independent experiments for EpiLCs (red open circles), epiblasts (red filled squares), and EpiSCs (blue filled squares), respectively, is shown on the $\log_2$ scale, with SDs. u.d., undetectable.

See also Figure S1 and Table S6.

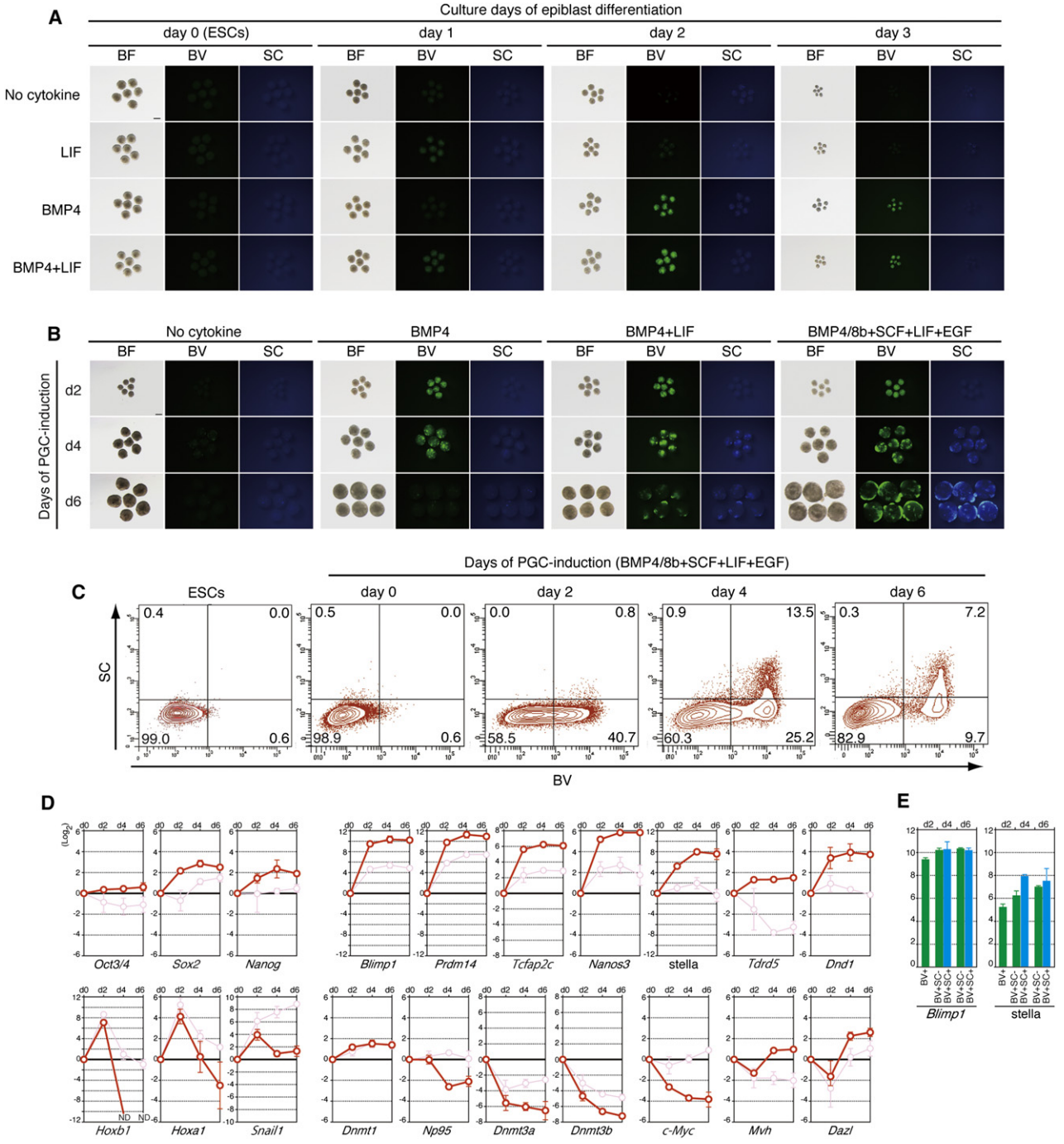

Figure 2. PGC-like Cell Induction from EpiLCs in Culture

(A) The effects of LIF, BMP4, or both on BV induction in ESCs and d1, 2, and 3 EpiLCs cultured for 2 days. Scale bar, 200 μm.

(B) The effects of BMP4, BMP4 and LIF, or BMP4, LIF, SCF, BMP8b, and EGF (full induction) on BVSC induction in the 6 day culture of the day (d) 2 EpiLCs. Scale bar, 200 μm.

(C) FACS analysis of the BVSC expression from d2 EpiLCs under the full induction condition during the 6 day culture.

(D) Gene expression dynamics during the PGCLC induction calculated as in Figure 1E. For each point, the average value from two independent experiments is plotted on the $\log_2$ scale, with standard deviations (SDs). Red circles and lines, values of BV or BVSC(+) cells (day 2 and days 4/6, respectively); pink circles and lines, values of BV(−) cells.

(E) *Blimp1* (left) and stella (right) expression levels with SDs in BV(+) (day 2) and BV(+)SC(−) (green bars) or BVSC(+) (blue bars) cells (days 4/6), determined as described in (D).

See also Figure S1, Figure S2, Figure S3, Figure S4, Figure S5, Figure S7, and Table S6.

the BV(+) cells (~9.8%) formed several tight clusters, some of which were positive for SC (BVSC, ~1.0%). On day 6, the aggregates developed further, but the BV(+) foci became much smaller (~0.4%) (Figure 2B and Figure S2B). When the d2 EpiLCs were cultured with BMP4 and LIF, on day 2, the aggregates showed strong BV positivity (~44.5%), and on day 4, the BV(+) cells formed tight and larger clusters (~42.0%), some of which exhibited SC (BVSC, ~7.4%). On day 6, the BVSC(+) foci (BV, ~5.2%; BVSC, ~1.0%) became smaller but did persist peripherally in the aggregates (Figure 2B and Figure S2B). From days 4 to 6, the BV-negative (BV-negative [−], negative or weak for BV defined by FACS) population exhibited rapid expansion (see below). When the d2 EpiLCs were cultured under the full induction condition (GK15 with BMP4, BMP8b, LIF, stem cell factor [SCF], and epidermal growth factor [EGF]), on day 2, the aggregates exhibited strong BV (~41.5%), and on day 4, BV(+) cells were located peripherally (~38.7%) and began to show explicit SC (BVSC, ~13.5%). On day 6, the whole aggregates expanded, and the BVSC(+) cells covered the aggregates peripherally (BV, ~16.9%; BVSC, ~7.2%) (Figures 2B and 2C and Figure S2B). Notably, when the d2 EpiLCs were cultured with BMP8b, SCF, LIF, and EGF or with SCF, LIF, and EGF but without BMP4, the aggregates looked similar to those cultured only with LIF, and no significant BV(SC) induction was observed (Figures S2B and S2C). These findings demonstrate that the d2 EpiLCs are induced into BVSC(+) PGC-like cells essentially by BMP4, and the maintenance/proliferation of the BVSC(+) cells is enhanced by LIF and more robustly by the combinatorial effects of LIF, SCF, BMP8b, and EGF.

The BVSC(+) areas were alkaline phosphatase (AP)-positive, and the BVSC(+) cells remained up to 10 days under the full induction condition (Figure S3). We were able to reproduce the induction of BVSC or P14V(+) PGC-like cells through the d2 EpiLCs from several independent ESC lines (Figure S4). In two-dimensional culture, we were unable to find a condition under which BV(SC)(+) cells are induced from the EpiLCs (data not shown).

We compared BVSC induction from d2 EpiLCs with that from the epiblasts. The structural development of the aggregates and the efficiency and dynamics of BVSC induction from the d2 EpiLCs were similar to those from the epiblasts (Figure S5A): under the full induction condition, on day 2, a majority of both the d2 EpiLCs and the epiblast cells were shifted toward the BV-positive state, and ~46% of the epiblast cells (as compared to ~41.5% of d2 EpiLCs) exhibited strong BV (Figures S5B and S5C), indicating that both cell types bear similar competence to express *Blimp1* in response to BMP4. On days 4/6, the efficiency and mode of the emergence of the BVSC(+) cells from both cell types were again similar, although the response of the epiblast cells appeared somewhat more cohesive (Figure S5C). These findings demonstrate that the d2 EpiLCs bear similar, if not identical, properties to the pregastrulating epiblast cells.

We evaluated the gene expression dynamics associated with the induction of PGC-like cells (hereafter called PGCLCs) from d2 EpiLCs by Q-PCR (Figure 2D). Whereas *Oct3/4* showed relatively constant expression in BV and BVSC(+) (day 2 and days 4/6, respectively) cells, *Sox2* and *Nanog* were significantly regained in these cells. Genes specifically upregulated upon PGC specification, including *Blimp1*, *Prdm14*, *Tcfap2c*, *Nanos3*, stella (*Dppa3*), *Tdrd5*, and *Dnd1*, were all highly elevated in BV(SC)(+) cells. In contrast, genes associated with a somatic mesodermal program, such as *Hoxa1*, *Hoxb1*, and *Snai1*, showed transient upregulation in BV(+) cells at day 2 but subsequently exhibited drastic repression in BVSC(+) cells at days 4/6. On the other hand, *Dnmt3a/3b*, *Np95 (Uhrf1)*, and *c-Myc* were monotonically downregulated. Genes associated with later germ cell development, *Mvh (Ddx4)* and *Dazl*, showed only a modest upregulation in BVSC(+) cells. Thus, the gene expression dynamics associated with PGCLC induction are very similar to those associated with PGC specification (Kurimoto et al., 2008; Saitou et al., 2002).

We noted that, at day 6, the level of endogenous stella mRNA in BV(+)SC(−) cells was similar to that in BVSC(+) cells (Figure 2E). Because the SC expression becomes eminent only after E9.5, 2.5 days later than the onset of stella expression (Ohinata et al., 2008; Saitou et al., 2002), this finding indicates that many of the BV(+)SC(−) cells at a later stage of induction express endogenous stella at a high level and thus should be considered established PGCLCs.

Global Transcription Profiles of EpiLCs and PGCLCs

To determine the global transcription dynamics for PGCLC induction, we isolated total RNAs from ESCs, d1/2/3 EpiLCs, EpiSCs, E5.75 epiblasts, and BVSC-positive PGCLCs at day 6 of induction and stella-EGFP(+) PGCs at E9.5 (Payer et al., 2006). We performed two sets of microarray hybridization: one with nonamplified RNAs from ESCs, d1/2/3 EpiLCs, EpiSCs, and PGCLCs and the other with amplified RNAs from ESCs, d2 EpiLCs, EpiSCs, E5.75 epiblasts, PGCLCs, and E9.5 PGCs.

Unsupervised hierarchical clustering (UHC) of nonamplified samples showed that two independent samples from ESCs, d1/2/3 EpiLCs, EpiSCs, and PGCLCs were clustered tightly together (Figure 3A), reflecting the reproducibility of the PGCLC induction. Principal component analysis (PCA) provided ESCs, d1, d2, and d3 EpiLCs with PC2 scores of progressively increasing values, suggesting that EpiLC induction from ESCs is a directional and progressive process (Figure 3B). EpiSCs were clustered distantly from the other samples (Figure 3A), indicating their divergence from the other cell types.

UHC of amplified samples showed that, first, two independent samples from all cell types were again clustered together, and second, d2 EpiLCs and PGCLCs were clustered most closely with E5.75 epiblasts and E9.5 PGCs, respectively, whereas EpiSCs were clustered distantly from the other cell types (Figure 3C). Scatter plot analysis demonstrated close similarities between d2 EpiLCs and E5.75 epiblasts and between PGCLCs and E9.5 PGCs and a relatively large difference between EpiSCs and E5.75 epiblasts (Figure 3D). We plotted all cell types in a three-dimensional space defined by three major parameters generated by PCA (Figure 3F). Notably, the pathway of PGCLC induction from d2 EpiLCs was parallel to that of E9.5 PGC formation from E5.75 epiblasts (Figure 3F). Furthermore, EpiSC derivation from epiblasts involves a discrete pathway (Figure 3F), reflected by a distinct PC1 (representing 61% of the total variance) score. These findings indicate strongly that PGCLC formation from ESCs through EpiLCs is a recapitulation of PGC formation from epiblasts.

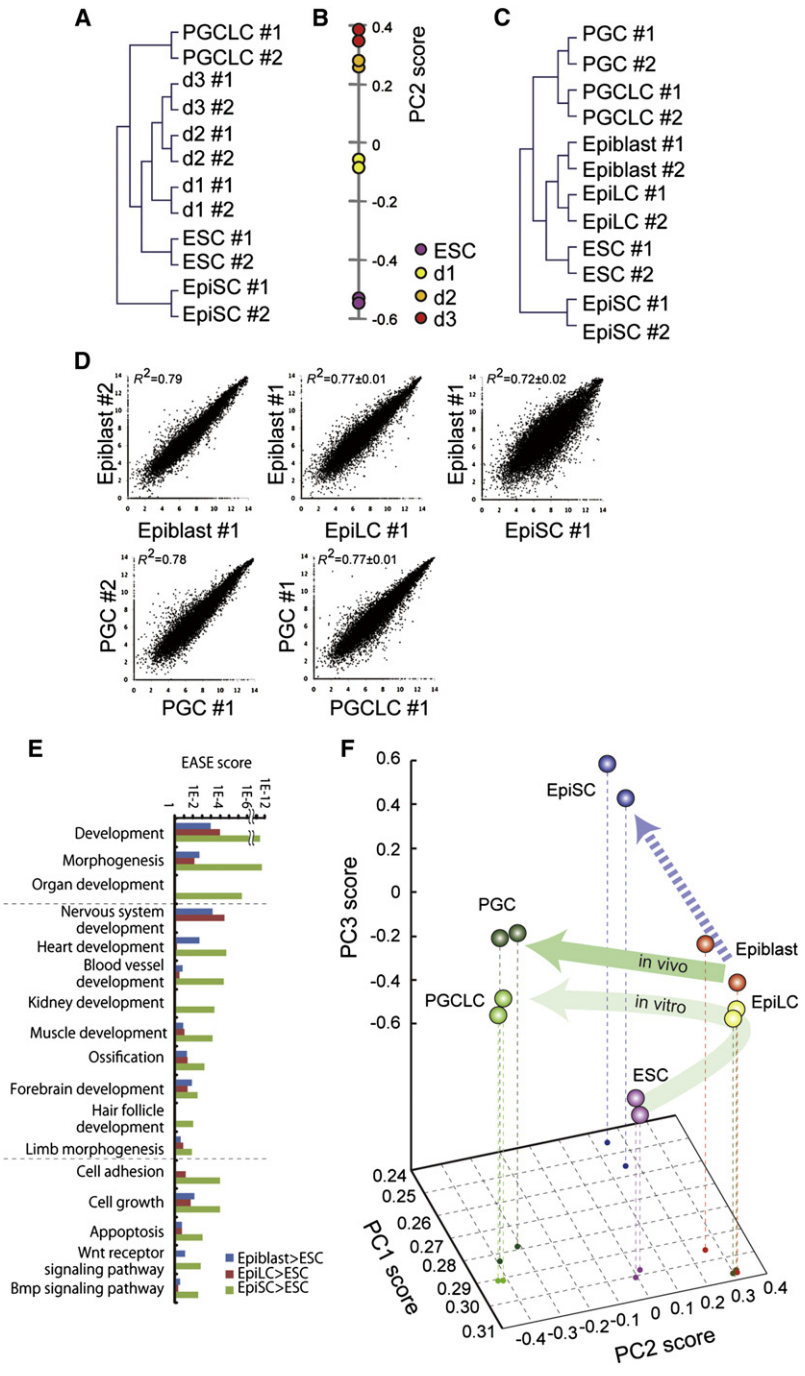

Figure 3. Global Transcription Profiles during PGCLC Induction

(A) Unsupervised hierarchical clustering (UHC) of non-amplified RNAs from ESCs; day (d) 1, d2, and d3 EpiLCs; EpiSCs; and PGCLCs.

(B) Scores of principal component (PC) 2 of ESCs and d1, d2, and d3 EpiLCs.

(C) UHC of amplified RNAs from ESCs, d2 EpiLCs, EpiSCs, E5.75 epiblasts, PGCLCs, and E9.5 PGCs.

(D) Comparison by scatter plots of transcriptome of E5.75 epiblasts with d2 EpiLCs and EpiSCs and of E9.5 PGCs with BVSC(+) PGCLCs at day 6. *R* represents the correlation coefficient.

(E) Functional categories overrepresented in genes upregulated in the epiblasts, EpiLCs, and EpiSCs, compared with ESCs.

(F) PCA of amplified RNAs from ESCs, d2EpiLCs, EpiSCs, E5.75 epiblasts, PGCLCs, and E9.5 PGCs.

See also Figure S7 and Table S1, Table S2, and Table S3.

We listed and classified the genes upregulated in E5.75 epiblasts, d2 EpiLCs, and EpiSCs relative to the levels in ESCs. EpiSCs upregulated more genes associated with the development of a variety of organ systems (heart, blood vessels, kidneys, muscle, and bone) than E5.75 epiblasts and d2 EpiLCs (Figure 3E and Table S2), demonstrating that EpiSCs acquire more developmentally advanced characteristics than E5.75 epiblasts and d2 EpiLCs. Major genes that are up- or downregulated in E5.75 epiblasts, d2 EpiLCs, and EpiSCs in comparison to ESCs, and in E9.5 PGCs and PGCLCs in comparison to epiblasts and EpiLCs, respectively, are listed in Table S2 and Table S3.

Epigenetic Profiles of the PGCLCs

We next evaluated the epigenetic profiles of PGCLCs. IF analysis revealed that BV(SC)(+) PGCLCs at day 6 appeared to have reduced H3K9me2 and cytosine methylation (5mC) and instead showed elevated H3K27me3 levels, as compared to non-PGCLCs (Figures 4A, 4B and 4D). To confirm this observation, we quantified the dynamics of H3K9me2, H3K27me3, and 5mC levels during the PGCLC induction by western/dot blot analysis. In ESC to EpiLC differentiation, the H3K9me2 and 5mC levels increased. In contrast, in EpiLC to PGCLC differentiation, they decreased significantly. Non-PGCLCs retained relatively high levels of H3K9me2 and 5mC (Figures 4C and 4E). On the other hand, in ESC to EpiLC differentiation, the H3K27me3 level decreased, and in EpiLC to PGCLC differentiation, it in turn increased. Non-PGCLCs retained a similar level of H3K27me3 to EpiLCs (Figure 4C). Thus, the dynamics of histone modification and 5mC changes during PGCLC formation are a recapitulation of those observed during PGC formation (Seki et al., 2005).

We determined the imprinting states of maternally (*Snrpn*, *Kcnq1ot1*) and paternally (*Igf2r*, *H19*) imprinted genes in PGCLCs. Whereas the PGCLCs did retain methylation of *Igf2r* and *Snrpn*, they appeared to have a slightly reduced level of methylation of *H19* and *Kcnq1ot1*, suggesting that PGCLCs may be initiating the process of imprint erasure (Figure 4F). A global decrease of 5mC with a relative maintenance of imprinting in PGCLCs is a characteristic that is consistent with that of migrating PGCs (Lee et al., 2002).

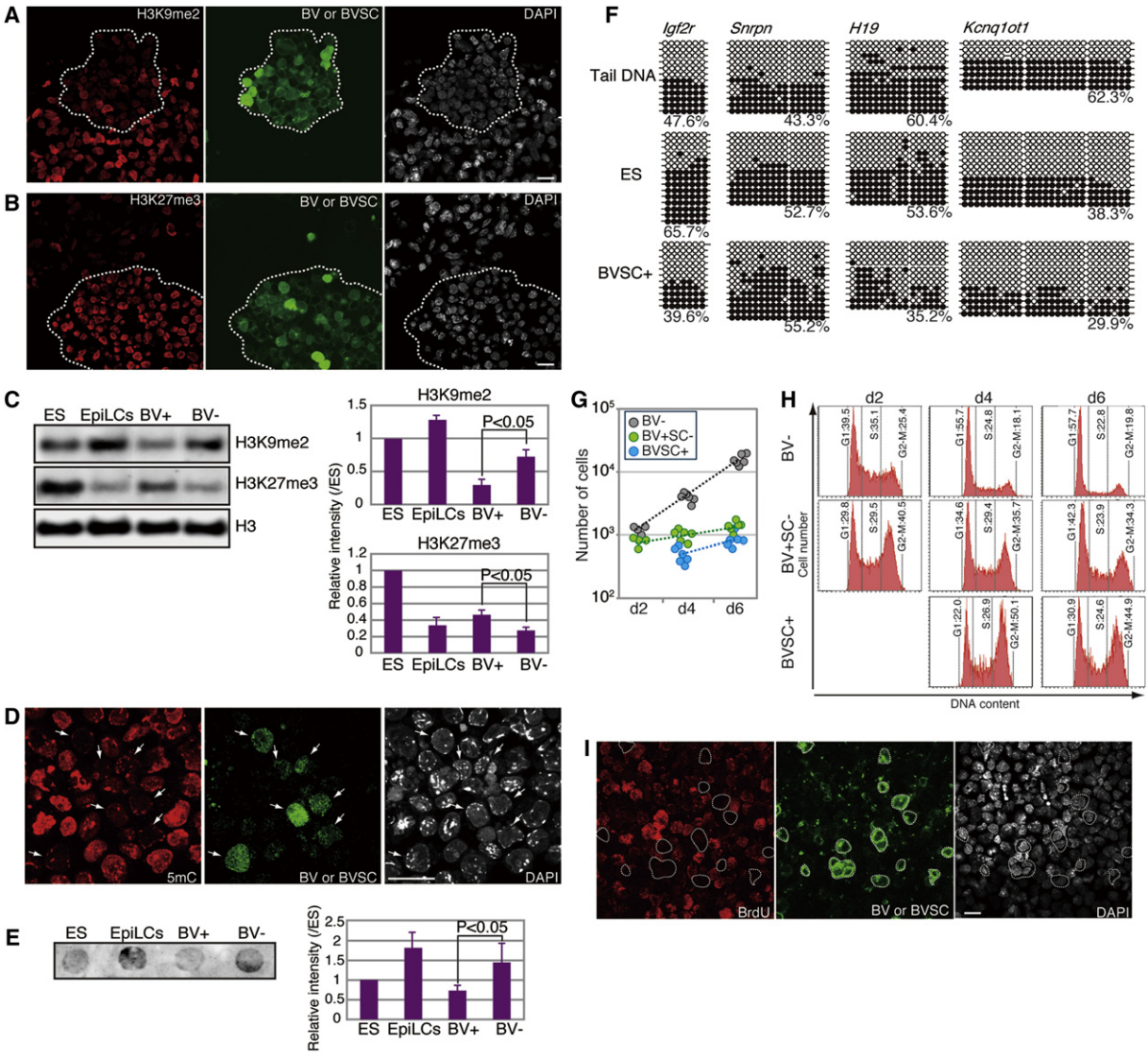

Figure 4. Epigenetic Properties and Cellular Dynamics of the PGCLCs

(A and B) IF analyses of H3K9me2 (A) and H3K27me3 (B) in PGCLCs under the full induction condition at day 6. Dotted lines delineate PGCLCs recognized by anti-GFP antibody staining. DAPI staining, on the right. Scale bar, 20 μm.

(C) Western blot analyses (left) of H3K9me2 and H3K27me3 in ESCs, d2 EpiLCs, and BV(+) or (−) cells induced for 6 days. Quantification of H3K9me2 and H3K27me3 levels using H3 levels as a standard is shown with the standard deviations (SDs) on the right.

(D) Immunofluorescence (IF) analysis of 5mC in PGCLCs performed as in (A) and (B). Arrows indicate PGCLCs. Scale bar, 20 μm.

(E) Dot blot analysis of 5mC performed as in (C). Quantification of the 5mC level using the ESC level as a standard is shown with SDs on the right.

(F) Bisulfite sequence analysis of 5mC of differentially methylated regions (DMRs) of the imprinted genes (*Igf2r*, *Snrpn*, *H19*, and *Kcnq1ot1*) in a wild-type mouse (top), the BVSC-ESCs (middle), and the day 6 BVSC(+) PGCLCs (bottom). White and black circles represent unmethylated and methylated CpG sequences, respectively.

(G) The numbers of BVSC(+) (blue circles), BV(+)SC(−) (green circles), and BV(−) (gray circles) cells per aggregate during the PGCLC induction. Each circle represents the average number of each cell type from 10 aggregates in four independent experiments.

(H) FACS analysis of the cell cycle states of BVSC(+), BV(+)SC(−), and BV(−) cells during the PGCLC induction.

(I) BrdU incorporation of the PGCLCs during the 6 hr culture on day 4 of induction. Dotted lines delineate PGCLCs recognized by anti-GFP antibody staining. Scale bar, 20 μm.

See also Table S4 and Table S6.

Dynamics of PGCLC Induction and Proliferation

We explored the dynamics of PGCLC induction and proliferation (Figure 4G and Table S4). At day 2 of PGCLC induction from aggregates of ~1000 EpiLCs, the average number of BV(+) cells was 783 (~39%), whereas that of BV(−) cells was 1225 (~61%). At day 4, the average number of BV(+) cells was 1415 (~26%),

Table 1. Colonization of the Donor Cells in the *W/W^v* Recipient Testes

Parental Cells	Transferred Population	No. of Testes Transplanted	No. of Cells Transplanted/Testis	No. of Testes with Teratoma (%)	No. of Testes with Spermatogenesis (%)	No. of Spermatogenesis Colonies in the Testis
BVSC ESCs	nonsorted cells	8	2.9×10^5	8/8 (100)	ND	ND
	BV (+) cells	6	1.1×10^4	0/6 (0)	3/6 (50)	4, 1, 1
AAG ESCs	nonsorted cells	6	2.4×10^4	6/6 (100)	ND	ND
	Integrin-β3, SSEA1 (+) cells	6	1.0×10^4	0/6 (0)	5/6 (83)	10, 8, 6, 3, 1
20D17 iPSCs	Integrin-β3, SSEA1 (+) cells	18	1.0×10^4	0/18 (0)	3/18 (17)	6, 2, 1
178B-5 iPSCs	Integrin-β3, SSEA1 (+) cells	6	1.0×10^4	2/6 (33)	0/4 (0)	0
492B-4 iPSCs	Integrin-β3, SSEA1 (+) cells	6	1.0×10^4	0/6 (0)	0/6 (0)	0

The donor PGC-like cells generated from the ESCs (BVSC and AAG) and the iPSCs (20D17, 178B-5, and 492B-4) were transferred into the *W/W^v* recipient testes through their seminiferous tubules. The colonization of the donor cells in the recipient testes is shown with the number (No.) of testes with teratoma formation or spermatogenesis and with the number of spermatogenesis colonies per testis. ND, not determined. See also Table S5.

among which 482 cells were SC(+) (~9%), whereas that of BV(−) cells was 3967 (~74%). At day 6, the average number of BV(+) cells was 2222 (~12%), among which 848 cells were SC(+) (~5%), whereas that of BV(−) cells was 15811 (~88%). The cell cycle analysis revealed that BV(+) cells, especially BVSC(+) cells at days 4/6, were enriched in the G2 phase, whereas BV(−) cells exhibited profiles similar to those of cycling somatic cells, especially at days 4/6 (Figure 4H). Consistently, PGCLCs showed little BrdU incorporation during the 6 hr culture on day 4 of induction, whereas non-PGCLCs actively incorporated BrdU (Figure 4I). Collectively, these data indicate that BV induction from EpiLCs is an efficient process, and presumably all of the BV(+) cells initiate stella expression thereafter (irrespective of their SC positivity; see above), but the induced BV(SC)(+) cells proliferate slowly (one to two divisions from day 2 to day 6), whereas BV (−) cells grow more rapidly (three to four divisions). The slow growth and the arrest at the G2 phase of the cell cycle are key characteristics of migrating PGCs (Seki et al., 2007), and the finding that PGCLCs bear equivalent properties provides further evidence that PGCLC formation is a reconstitution of PGC formation.

Spermatogenesis and Normal Offspring from PGCLCs

A cell's ability to contribute to spermatogenesis is the most stringent index of whether it has become a male germ cell. We next examined whether the PGCLCs undergo proper spermatogenesis by transplanting them into the seminiferous tubules of *W/W^v* neonatal mice lacking endogenous germ cells (Chuma et al., 2005). We induced the PGCLCs for 6 days, transplanted dissociated single cells from the entire aggregates or the FACS-sorted BV(+) cells (~10^4 cells/testis), and evaluated the recipients after 10 weeks. All of the testes transplanted with nonsorted cells developed teratomas, but those transplanted with the BV(+) cells did not (Table 1). Instead, three out of six testes transplanted with the BV(+) cells harbored seminiferous tubules with proper spermatogenesis: these tubules contained dark central sections corresponding to spermiation and were much thicker than those without spermatogenesis (Figure 5A and Table 1). Indeed, the thick tubules contained abundant spermatozoa with normal morphology and showed a robust wave of spermatogenesis, whereas the thin tubules contained only Sertoli cells (Figure 5A). The efficiency of the colonization of the PGCLCs was comparable to that of PGCs in vivo (Chuma et al., 2005; Ohinata et al., 2009).

We fertilized the oocytes with the spermatozoa derived from PGCLCs by intracytoplasmic sperm injection (ICSI). The resultant zygotes developed normally, and by the blastocyst stage, embryos from PGCLC-derived sperm exhibited strong expression of SC derived from the donor genome (Figure 5B). We transferred the embryos to foster mothers, which gave rise to grossly healthy offspring with normal placentas and imprinting patterns (Figures 5C, 5D, and 5F). The BV and SC transgenes were positive in 13 and 7 of 21 offspring, respectively (Figure 5C), consistent with the transmission of the transgenes through haploid donor spermatozoa. The male and female offspring from the PGCLCs developed normally and grew into fertile adults (Figures 5D and 5E and Table S5). These findings demonstrate that the PGCLCs are comparable to PGCs in their function as male germ cells.

Identification of Surface Markers for PGCLC Isolation

Identification of surface markers delineating a pure population of PGCLCs is essential for isolating PGCLCs bearing no transgenic reporters, such as those induced from iPSCs or ESCs from various mammalian species, including humans (Saitou and Yamaji, 2010). We screened surface markers (SSEA1, PECAM1, EPCAM, N-cadherin, Integrin-β3, Integrin-αV, CXCR4, and KIT) and their combinations to identify those that define the BV(+) population. When aggregates of BVSC d2 EpiLCs induced for 6 days were FACS sorted by SSEA1 and Integrin-β3, they were divided into three major subpopulations (P1 [SSEA1 high, Integrin-β3 high], P2 [SSEA1 high, Integrin-β3 low], and P3 [SSEA1 low, Integrin-β3 high/low]). Notably, more than 99% of the cells in P1 were BV(+), whereas only 1.2% and 1.7% of the cells in P2 and P3, respectively, contained BV(+) cells (Figure 6A), indicating that P1 is nearly identical to the BV(+) population.

We induced ESCs bearing *Acro/Act-EGFP* (AAG) transgenes (Ohta et al., 2000) into PGCLCs and FACS sorted the day 6 aggregates by SSEA1 and Integrin-β3. Although the sorting pattern of these aggregates was somewhat different than that of the aggregates from BVSC ESCs, we identified three similar subpopulations (Figure 6B). We compared the expression levels of the 20 genes analyzed in Figure 2D between these subpopulations and the BV(+) PGCLCs. The expression levels of the 20 genes in P1 correlated well with those in BV(+) PGCLCs (R^2 = 0.80), whereas those in the other two subpopulations showed poor correlation (Figure 6B).

To examine whether the P1 subpopulation from AAG ESCs contributes to the spermatogenesis, we transplanted them, as well as the whole population, into the seminiferous tubules of W/W^v mice and evaluated the recipients after 8 weeks. We found teratomas in all of the testes transplanted with the whole population, whereas no teratomas were detected in the testes with the P1 subpopulation, and indeed, five out of six testes demonstrated proper spermatogenesis with GFP fluorescence by the AAG transgenes (Figures 6C–6G and Table 1). With ICSI followed by embryo transfer, the resultant sperm contributed to fertile offspring (Figure 6H and Table S5). These findings demonstrate that the sorting by SSEA1 and Integrin-β3 purifies PGCLCs with essentially no contamination of teratogenic cells, establishing the formation and purification of PGCLCs from ESCs without relevant transgenic markers.

PGCLCs, Spermatogenesis, and Offspring from iPSCs

Finally, we explored whether the germ cell specification pathway would be reconstituted by iPSCs. We used three iPSC lines, 20D17 (Okita et al., 2007), 178B-5 (Nakagawa et al., 2008), and 492B-4 (Okita et al., 2008), all bearing *Nanog-EGFP* (NG) transgenes. They all expressed NG in the ground state and exhibited differentiation into EpiLCs with proper morphology and NG downregulation (Figures S6A, S6D, and S6G). Upon PGCLC induction, they showed NG upregulation as early as day 2, and NG-positive cells formed clusters around the periphery of the aggregates at days 4/6 (Figures S6B, S6E, and S6H).

We FACS sorted the induced aggregates at day 6 by SSEA1 and Integrin-β3. The sorting patterns of the three lines were somewhat different from one another, and that of the 20D17 line was more similar to those of the ESC lines (Figure 6I and Figures S6C, S6F, and S6I). In aggregates of the 20D17 line, NG-positive cells represented ~57% (Figure S6C). Consistent with the characteristics of migrating PGCs, the P1 subpopulation contained both NG-high and NG-low cells (Figure S6C) (Yamaguchi et al., 2005). On the other hand, the P2 subpopulation was rich in NG-high cells and was thus probably an undifferentiated population (Figure S6C).

The expression levels of the 20 genes analyzed in Figure 2D in the P1 subpopulation from the 20D17 line exhibited a prominent correlation with those in BV(+) PGCLCs (R^2 = 0.96), whereas those in the other two subpopulations showed a poor correlation (Figure 6I). We transplanted the P1 cells from the three lines into the seminiferous tubules of W/W^v mice and evaluated the recipients after 10 weeks. No testes with cells from the 178B-5 or 492B-4 lines showed spermatogenesis, and two with the 178B-5 cells resulted in teratomas (Table 1). Remarkably, 3 out of 18 testes with the cells from the 20D17 line exhibited proper spermatogenesis, and we observed no teratomas in the recipients of this line (Figure 6J and Table 1). With ICSI followed by embryo transfer, the resultant sperm contributed to fertile offspring (Figure 6K and Table S5). Notably, some of the offspring died prematurely, apparently due to tumors around the neck region (data not shown), similar to those observed in some of the F1 offspring of the 20D17 chimeras (Okita et al., 2007). These findings demonstrate that, although iPSCs exhibit different induction properties depending on the lines, they can nonetheless form PGCLCs with proper function.

DISCUSSION

We induced pregastrulating epiblast-like cells, EpiLCs, from ground state ESCs that were maintained by 2i and LIF under a serum- and feeder-free condition. ESCs cultured in the presence of serum show substantial heterogeneity (Hayashi et al., 2008) and were inadequate for the uniform induction of EpiLCs (data not shown). EpiLC induction involves ActA and bFGF, the same cytokines that are required for the derivation of EpiSCs, as well as the addition of 1% KSR. d2 EpiLCs were robustly induced into the PGC fate, but ESCs, d1/3 EpiLCs, and EpiSCs were not (Figure 2). This should be a reflection of the fact that only epiblasts at E5.5~E6.0 serve as an efficient precursor for the PGC fate (Ohinata et al., 2009). The self-renewing EpiSCs show a significant heterogeneity (Figure S1) (Hayashi et al., 2008) and a substantially different transcriptome from the original epiblasts (Figure 3), indicating that continuous stimulation by ActA and bFGF stabilizes the properties of the epiblast-derived cells (EpiSCs) in a condition that is different than their original states. It is of note that, when EpiSCs were reverted into ESC-like cells (Greber et al., 2010), they were induced into PGCLCs through EpiLCs (Figure S7).

Wnt3 is required for competence for the PGC fate (Ohinata et al., 2009). EpiLCs express *Wnt3* at a level similar to that in the epiblasts (Figure 1E), and this would confer the PGC competence to EpiLCs. Addition of exogenous Wnt3a during EpiLC induction, however, had no additive effects on the properties of EpiLCs or their capacity to form PGCLCs (data not shown). Notably, EpiSCs also express a high level of *Wnt3* yet are inefficient for the PGC fate (Figure 1E and Figure S1). The competence for the PGC fate would therefore be a complex trait governed by both the signaling and epigenetic states of the cells. The precise mechanism conferring the competence for the PGC fate warrants further investigation.

The derivation of EpiLCs has critical implications in stem cell biology. For example, the ESC to EpiLC differentiation serves as a model for the investigation of the genetic and epigenetic mechanisms underlying the ICM to epiblast differentiation. A comprehensive comparison of genetic and epigenetic properties among ESCs, EpiLCs, and EpiSCs would lead to a better understanding of the naive and primed pluripotency (Nichols and Smith, 2009). More practically, EpiLCs may serve as a starting material for the induction of other lineages derived from the epiblast. The EpiLCs are a transient entity and undergo relatively large-scale cell death after day 2 of induction via an unknown mechanism. They have been difficult to maintain longer than

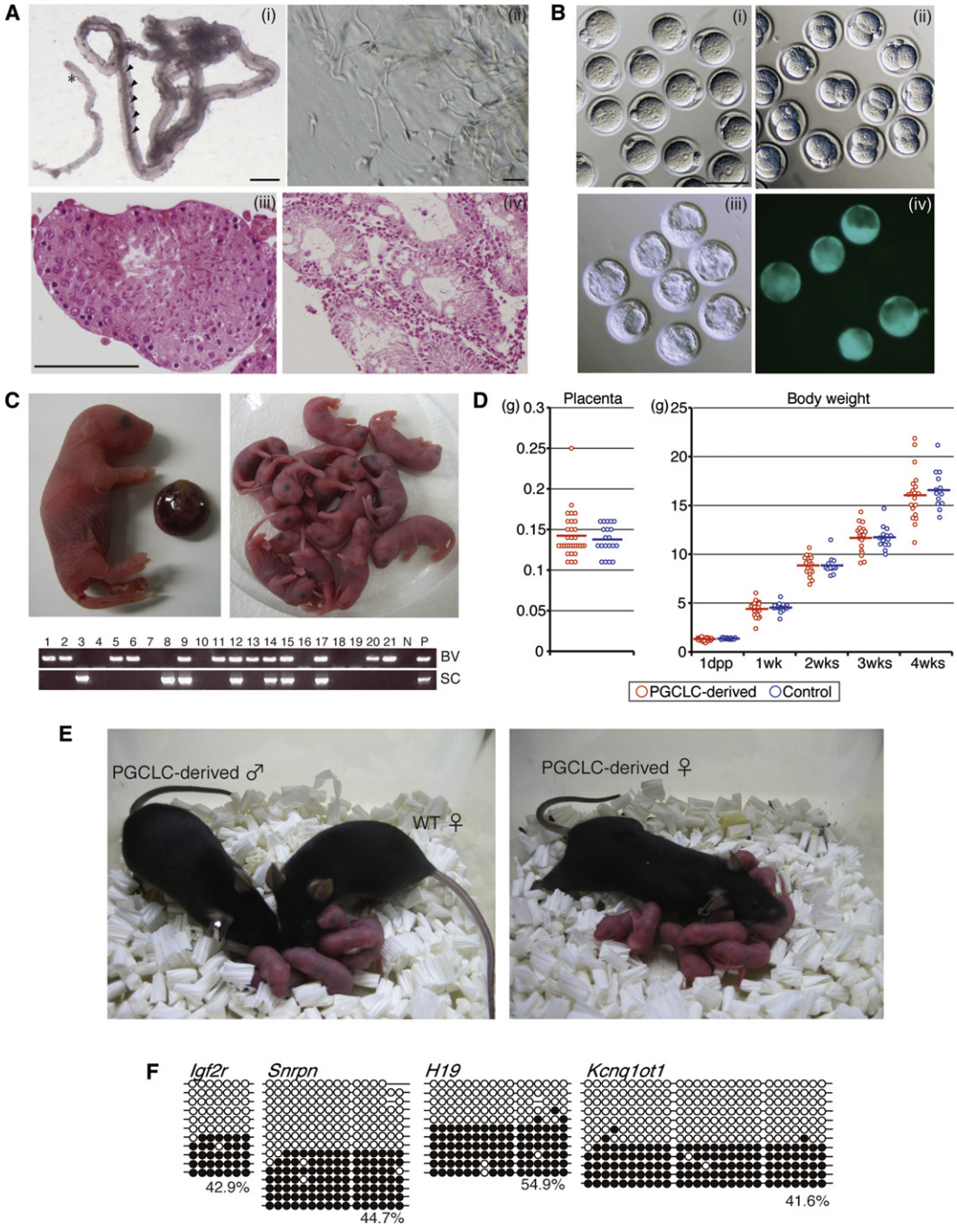

Figure 5. Spermatogenesis and Healthy Offspring from PGCLCs

(A) (i) The seminiferous tubules transplanted with the PGCLCs, showing (right) or not showing (left) spermatogenesis. Arrowheads indicate spermiated areas of the tubule. Scale bar, 500 μm. (ii) Spermatozoa derived from the PGCLCs. Scale bar, 20 μm. (iii, iv) Hematoxylin and eosin-stained sections of the tubules with (iii) or without (iv) spermatogenesis. Scale bar, 100 μm.

(B) The pronucleus stage embryos (i), the two-cell embryos (ii), and the blastocysts (iii) with SC expression (iv) derived from spermatozoa from the PGCLCs. Scale bar, 100 μm.

(C) The offspring with normal placenta (left) derived from spermatozoa from the PGCLCs. Genotyping of the offspring for BV and SC transgenes is shown at the bottom.

(D) Weights (gram) of placentas (left) and development of the body weights (right) of offspring from the PGCLC-derived sperm (red circles) and from the wild-type sperm (blue circles). The mean values are indicated as bars.

(E) A male (left) and female (right) offspring from PGCLC-derived spermatozoa with full fertility.

3 days and differentiate into mesenchyme-like cells after passaging (data not shown). They thus may require additional cytokines or a different condition for their maintenance. Nonetheless, EpiLC derivation from ESCs is a straightforward process, providing a strategy for in vitro reconstitution of lineage specification.

A previous report showed that ESCs can be converted into early primitive ectoderm-like cells (EPLCs) (Rathjen et al., 1999). In that study, the EPLCs were shown to self-renew and bear epiblast-like gene expression and morphology. In addition, like the epiblasts, they were unable to contribute to chimeras when injected into blastocysts. However, their derivation involved serum and an undefined HepG2-conditioned medium, and their further properties, such as genome-wide gene expression, were not investigated. Therefore, whether EPLCs might truly represent a pregastrulating epiblast-like state and serve as a suitable precursor for PGC-like cells will require further investigation.

Upon PGCLC induction, a majority of d2 EpiLCs initiate BV expression, with ~40% acquiring strong BV levels on day 2 (Figure 2C, Figure S2, and Figure S5). We therefore assume that, upon induction, a majority of d2 EpiLCs are directed toward the PGC fate, and those (~40%) that acquire *Blimp1* at a sufficient level succeed in progressing toward PGCLCs with appropriate genetic, epigenetic, and cellular properties, whereas those that fail to do so, due to some stochastic/physical parameter or intrinsic difference, result in a nongerm cell trait. In good agreement with this assumption, the BV(SC)(+) cell induction from the epiblasts ex vivo exhibited similar dynamics (Figure S5). Furthermore, among the cells originated from the most proximal epiblasts, only those that acquire high, but not low, levels of *Blimp1* develop into PGCs in vivo (Kurimoto et al., 2008). We noted, however, that the response of the epiblasts was somewhat more cohesive than that of EpiLCs (Figure S5). In part, this may be because EpiLCs are dissociated into single cells and reaggregated upon induction, whereas epiblasts are tightly adhering, perhaps highly synchronized, epithelial structures at the outset. Further elaboration of the EpiLC/PGCLC induction protocol may lead to more efficient generation of PGCLCs.

The identification of surface markers for PGCLCs (SSEA-1 and Integrin-β3) has enabled the induction and purification of PGCLCs with a capacity for proper spermatogenesis from iPSCs (Figure 6). Upon PGCLC induction, the three iPSC lines exhibited different differentiation properties (Figure 6 and Figure S6). Consistent with the fact that 20D17 has the highest capacity for germline transmission among the three lines (Okita et al., 2007) (K. Okita and S. Yamanaka, personal communication), only the PGCLCs from 20D17 exhibited spermatogenesis in our trials (Figure 6 and Table 1). Indeed, it has been shown recently that the efficiency of germline transmission of iPSCs depends highly on the introduction of the *Myc* transgene (Nakagawa et al., 2010): 20D17 was derived by retroviral stable transduction of *c-Myc*, whereas the other two lines were derived without, or by transient expression of, *c-Myc* (Nakagawa et al., 2008; Okita et al., 2007, 2008). Thus, the efficiency of the contribution to the spermatogenesis of the PGCLCs derived from the iPSCs depends on the original properties of the iPSC lines.

The surface marker identification for PGCLCs may also be useful for the purification of PGCLCs from ESCs of other mammalian species, including humans. It should be noted that hESCs have substantially different properties than mESCs but exhibit characteristics similar to mEpiSCs (Brons et al., 2007; Tesar et al., 2007; Thomson et al., 1998). However, hESCs and mEpiSCs do show differences in their gene expression, transcription factor dependency, and responses to signaling molecules (Chia et al., 2010; Greber et al., 2010). Thus, to establish a defined methodology for inducing proper PGCLCs from hESCs, careful studies on the nature of hESCs and on the mechanism of PGC specification in primate models would be critical.

The mechanism for PGC specification/development has been difficult to explore, mainly because PGCs are small in number and refractory to proliferation in vitro (Saitou and Yamaji, 2010). Our culture system readily allows the generation of PGCLCs in a relatively large number (~10^5–10^6) and thus should serve as a foundation for elucidating areas of germ cell biology that have thus far been unexplored due to material limitations, e.g., the biochemical properties of key proteins involved in PGC specification/proliferation/survival, the mechanism of epigenetic reprogramming in PGCs, etc. Continued investigations aimed at in vitro reconstitution of germ cell development, including the induction of female PGCLCs and their descendants, will be crucial for a more comprehensive understanding of germ cell biology in general, as well as for the advancement of reproductive technology and medicine.

EXPERIMENTAL PROCEDURES

The experimental procedures for animal experiments, FACS analysis, Q-PCR, microarray analysis, bisulfite sequencing, genotyping, AP staining, immunohistochemistry, western/dot blot analysis, and BrdU incorporation are available in the Extended Experimental Procedures.

ESC Derivation and Culture

The blastocysts bearing the BVSC and ROSA transgenes (B6;129S-Gt[ROSA]26Sor/J; the Jackson Laboratory) were flushed out from the uterus at E3.5 and placed and cultured in a well of a 96-well plate in N2B27 medium with 2i (PD0325901, 0.4 μM: Stemgent, San Diego, CA; CHIR99021, 3 μM: Stemgent) and LIF (1000 u/ml) on mouse embryonic feeders (MEFs) (Ying et al., 2008). The expanded ESC colonies were passaged by dissociating with TrypLE (Invitrogen). Until passage 4, the ESCs were maintained on MEFs. At passage 4, the ESCs were stocked in Cell Banker 3 solution (ZENOAQ). Thereafter, male ESCs were thawed, cultured, and maintained feeder-free on a dish coated with poly-L-ornithine (0.01%; Sigma) and laminin (10 ng/ml; BD Biosciences). The ESCs bearing the AAG transgenes (129Sv × C57BL/6) (Ohta et al., 2000) were derived by a standard ESC derivation procedure and were adapted to the 2i+LIF, feeder-free culture condition. The male iPSCs (MEF-Ng-20D-17, MEF-Ng-178B-5, and MEF-Ng-492B-4) (Nakagawa et al., 2008; Okita et al., 2007, 2008) were obtained from RIKEN BRC and were adapted to the 2i+LIF, feeder-free culture condition.

(F) Bisulfite sequence analysis of 5mC of DMRs of the imprinted genes (*Igf2r*, *Snrpn*, *H19*, and *Kcnq1ot1*) in the offspring derived from spermatozoa from the PGCLCs. White and black circles represent unmethylated and methylated CpG sequences, respectively.
See also Table S5 and Table S6.

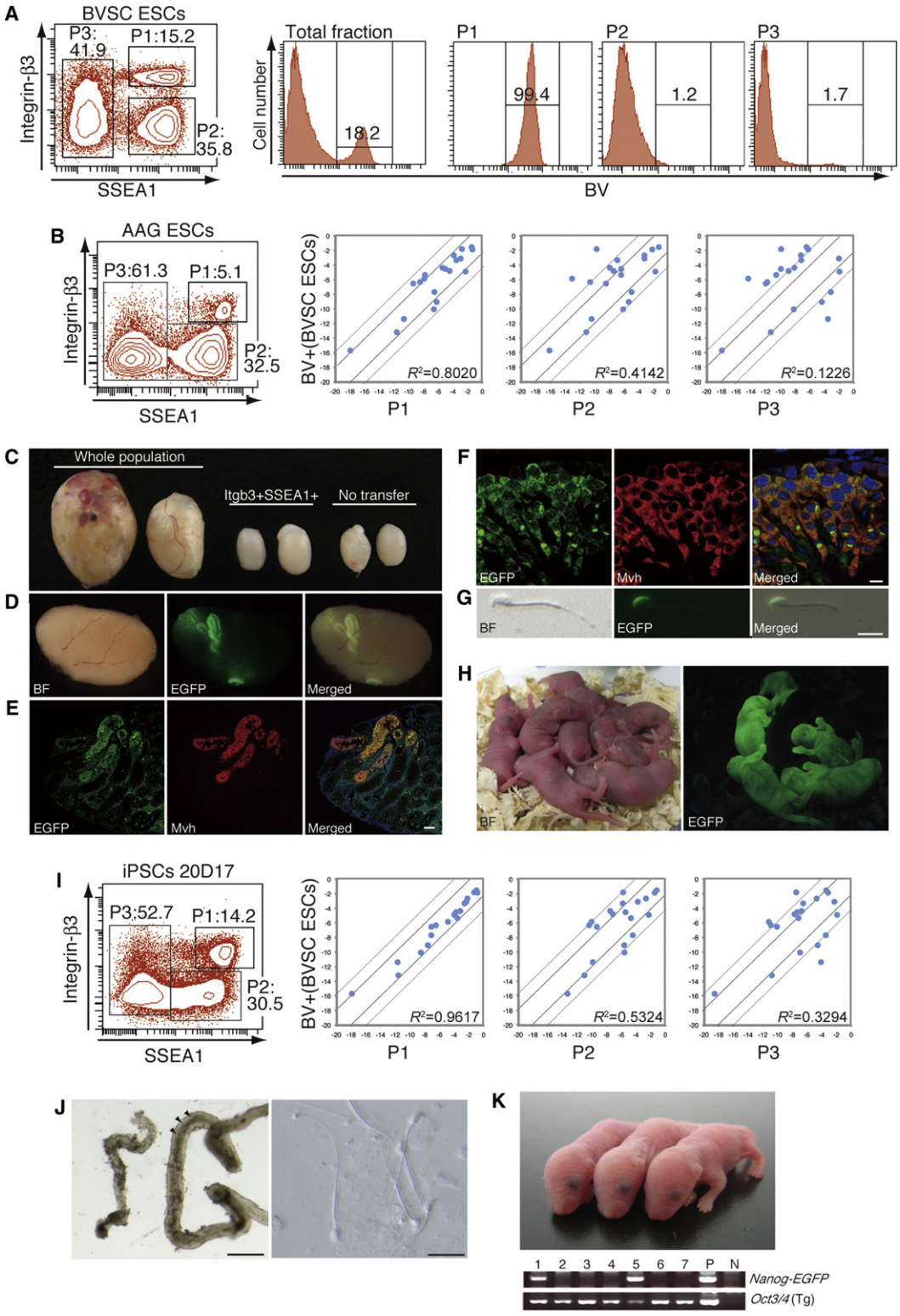

Figure 6. Induction and Purification of PGCLCs with Capacity for Spermatogenesis from ESCs and iPSCs without Germ Cell Reporters

(A) FACS sorting by SSEA1 and Integrin-β3 of day 6 aggregates for the PGC fate from BVSC ESCs (left). The SSEA1/Integrin-β3 high P1 subpopulation is nearly identical to the BV(+) subpopulation (right). Numbers represent the percentages of each subpopulation.

(B) FACS sorting by SSEA1 and Integrin-β3 of day 6 aggregates for the PGC fate from AAG ESCs (left). Comparison of the expression levels of the 20 genes (those analyzed in Figure 2D) in each subpopulation (P1, P2, and P3) with those in BV(+) cells (right). *R* represents the correlation coefficient.

EpiSC Derivation and Culture

The EpiSCs were derived from E5.75 epiblasts on MEFs in N2B27 medium containing activin A (20 ng/ml; Peprotech), bFGF (12 ng/ml; Invitrogen), and KSR (20%; Invitrogen) (Hayashi and Surani, 2009). The cells were passaged every 3 days by dissociating with collagenase IV (1 mg/ml; Invitrogen) as cell clumps, and the cells bearing the typical morphology of EpiSCs were established after around 10 passages.

Induction of EpiLCs and PGCLCs

The EpiLCs were induced by plating 1.0 × 10^5 ESCs/iPSCs on a well of a 12-well plate coated with human plasma fibronectin (16.7 μg/ml) in N2B27 medium containing activin A (20 ng/ml), bFGF (12 ng/ml), and KSR (1%). The medium was changed every day. The PGCLCs were induced under a floating condition by plating 1.0 × 10^3 EpiLCs in a well of a low-cell-binding U-bottom 96-well plate (NUNC) in a serum-free medium (GK15; GMEM [Invitrogen] with 15% KSR, 0.1 mM NEAA, 1 mM sodium pyruvate, 0.1 mM 2-mercaptoethanol, 100 U/ml penicillin, 0.1 mg/ml streptomycin, and 2 mM L-glutamine) in the presence of the cytokines BMP4 (500 ng/ml; R&D Systems), LIF (1000 u/ml; Invitrogen), SCF (100 ng/ml; R&D Systems), BMP8b (500 ng/ml; R&D Systems), and EGF (50 ng/ml; R&D Systems).

Transplantation of the PGCLCs into Seminiferous Tubules of Neonatal *W/W^v* Mice and Intracytoplasmic Sperm Injection

The whole aggregates (~192 [two 96-well plates] aggregates per experiment) of the PGCLC induction were dissociated into single cells by TrypLE treatment (Invitrogen). Recipient animals (neonatal [7- to 9-day-old] *W/W^v* mice lacking endogenous spermatogenesis [Mintz and Russell, 1957] from a WB × C57BL/6 F1 background [SLC]) were induced into hypothermic anesthesia on ice, and the donor cell suspension (the whole-cell dissociates or the FACS-sorted cells [~2 μl] [Table 1]) was injected into the efferent duct of each testis (Ogawa et al., 1997). The recipient animals were returned to their littermates after surgery.

The spermatozoa derived from the PGCLCs were prepared from the seminiferous tubules of recipient testis at 8–10 weeks after transplantation. In brief, the seminiferous tubules were isolated from the recipient testis, and those with dark central areas corresponding to spermiation or with GFP fluorescence from the *Acro/Act-EGFP* transgenes were located under a dissection microscope. These tubules were minced gently with scissors and dissociated to obtain the spermatogenic cell suspension. The cell suspension was kept at 4°C until ICSI. The ICSI was performed essentially as described previously (Kimura and Yanagimachi, 1995).

Reversion of EpiSCs into ESC-like Cells

Reversion of EpiSCs into ESC-like cells was performed essentially as described previously (Greber et al., 2010). EpiSCs maintained on MEFs in N2B27 medium containing activin A (20 ng/ml; Peprotech), bFGF (12 ng/ml; Invitrogen), and KSR (20%; Invitrogen) were passaged as clumps onto a dish without MEFs in N2B27 medium containing 2i, LIF, and KSR (20%). After 2 days, the cells were passaged as single cells in the same medium. After a further 3 days, the cells were passaged as single cells in N2B27 medium containing only 2i and LIF. After 8 days, the growing ESC-like colonies were picked up and passaged every 2–3 days. The reverted ESC-like cells were established after several passages.

PGC-like Cell Induction from the Epiblasts

PGC-like cell induction from the epiblasts was performed as described previously (Ohinata et al., 2009).

ACCESSION NUMBERS

The Gene Expression Omnibus (GEO) database accession number for the microarray data reported in this study is GSE30056.

SUPPLEMENTAL INFORMATION

Supplemental Information includes Extended Experimental Procedures, seven figures, and six tables and can be found with this article online at doi:10.1016/j.cell.2011.06.052.

ACKNOWLEDGMENTS

We thank J. Nichols for her advice on the ground state ESC culture. We are grateful to K. Okita and S. Yamanaka for the information on germline transmission of the three iPSC lines. We also thank K. Kabashima, H. Tanizaki, K. Takakura, S. Chuma, and N. Nakatsuji for their support with the FACS analysis; A. Fukunaga for her help with bisulfate sequence analysis; and Y. Toda for his help with the histology. S.A. is a JSPS research fellow. This study was supported, in part, by a Grant-in-Aid from the Ministry of Education, Culture, Sports, Science, and Technology of Japan; by JST-CREST; by the Takeda Science Foundation; and by the Uehara Memorial Foundation.

Received: February 1, 2011
Revised: May 10, 2011
Accepted: June 28, 2011
Published online: August 4, 2011

REFERENCES

Brons, I.G., Smithers, L.E., Trotter, M.W., Rugg-Gunn, P., Sun, B., Chuva de Sousa Lopes, S.M., Howlett, S.K., Clarkson, A., Ahrlund-Richter, L., Pedersen, R.A., and Vallier, L. (2007). Derivation of pluripotent epiblast stem cells from mammalian embryos. Nature *448*, 191–195.

Chia, N.Y., Chan, Y.S., Feng, B., Lu, X., Orlov, Y.L., Moreau, D., Kumar, P., Yang, L., Jiang, J., Lau, M.S., et al. (2010). A genome-wide RNAi screen reveals determinants of human embryonic stem cell identity. Nature *468*, 316–320.

Chuma, S., Kanatsu-Shinohara, M., Inoue, K., Ogonuki, N., Miki, H., Toyokuni, S., Hosokawa, M., Nakatsuji, N., Ogura, A., and Shinohara, T. (2005). Spermatogenesis from epiblast and primordial germ cells following transplantation into postnatal mouse testis. Development *132*, 117–122.

Daley, G.Q. (2007). Gametes from embryonic stem cells: a cup half empty or half full? Science *316*, 409–410.

Evans, M.J., and Kaufman, M.H. (1981). Establishment in culture of pluripotential cells from mouse embryos. Nature *292*, 154–156.

(C) Testes of *W/W^v* mice transplanted with the whole population (left), the P1 subpopulation (middle), and no cells (right) of aggregates of day (d) 2 EpiLCs with AAG transgenes induced for the PGC fate for 6 days.
(D) Spermatogenic colonies in a *W/W^v* testis transplanted with the P1 subpopulation. BF, bright-field image.
(E and F) Immunofluorescence (IF) analysis of EGFP and Mvh expression in a spermatogenic colony in (D). Scale bars: (E) 100 μm, (F) 10 μm.
(G) A spermatazoan derived from AAG ESCs. Scale bar, 10 μm.
(H) The offspring derived from spermatozoa from AAG ESCs. About half of them show GFP fluorescence from AAG transgenes (right).
(I) FACS sorting by SSEA1 and Integrin-β3 of day 6 aggregates for the PGC fate derived from iPSCs (20D17) (left). Comparison of expression levels of the 20 genes (those analyzed in Figure 2D) in each subpopulation (P1, P2, and P3) with those in BV(+) cells (right). *R* represents the correlation coefficient.
(J) (Left) The seminiferous tubules transplanted with the PGCLCs from iPSCs, showing (right) or not showing (left) spermatogenesis. Arrowheads indicate spermiated areas of the tubule. Scale bar, 500 μm. (Right) Spermatozoa derived from the PGCLCs from iPSCs. Scale bar, 20 μm.
(K) The offspring derived from spermatozoa from iPSCs. Genotyping of the offspring for NG and *Oct3/4* (for iPSC generation) transgenes is shown at the bottom.
See also Figure S6, Table S5, and Table S6.

Ginsburg, M., Snow, M.H., and McLaren, A. (1990). Primordial germ cells in the mouse embryo during gastrulation. Development *110*, 521–528.

Greber, B., Wu, G., Bernemann, C., Joo, J.Y., Han, D.W., Ko, K., Tapia, N., Sabour, D., Sterneckert, J., Tesar, P., and Schöler, H.R. (2010). Conserved and divergent roles of FGF signaling in mouse epiblast stem cells and human embryonic stem cells. Cell Stem Cell *6*, 215–226.

Guo, G., Yang, J., Nichols, J., Hall, J.S., Eyres, I., Mansfield, W., and Smith, A. (2009). Klf4 reverts developmentally programmed restriction of ground state pluripotency. Development *136*, 1063–1069.

Han, D.W., Tapia, N., Joo, J.Y., Greber, B., Araúzo-Bravo, M.J., Bernemann, C., Ko, K., Wu, G., Stehling, M., Do, J.T., and Schöler, H.R. (2010). Epiblast stem cell subpopulations represent mouse embryos of distinct pregastrulation stages. Cell *143*, 617–627.

Hayashi, K., and Surani, M.A. (2009). Self-renewing epiblast stem cells exhibit continual delineation of germ cells with epigenetic reprogramming in vitro. Development *136*, 3549–3556.

Hayashi, K., Lopes, S.M., Tang, F., and Surani, M.A. (2008). Dynamic equilibrium and heterogeneity of mouse pluripotent stem cells with distinct functional and epigenetic states. Cell Stem Cell *3*, 391–401.

Kimura, Y., and Yanagimachi, R. (1995). Intracytoplasmic sperm injection in the mouse. Biol. Reprod. *52*, 709–720.

Kurimoto, K., Yabuta, Y., Ohinata, Y., Shigeta, M., Yamanaka, K., and Saitou, M. (2008). Complex genome-wide transcription dynamics orchestrated by Blimp1 for the specification of the germ cell lineage in mice. Genes Dev. *22*, 1617–1635.

Lawson, K.A., Dunn, N.R., Roelen, B.A., Zeinstra, L.M., Davis, A.M., Wright, C.V., Korving, J.P., and Hogan, B.L. (1999). Bmp4 is required for the generation of primordial germ cells in the mouse embryo. Genes Dev. *13*, 424–436.

Lee, J., Inoue, K., Ono, R., Ogonuki, N., Kohda, T., Kaneko-Ishino, T., Ogura, A., and Ishino, F. (2002). Erasing genomic imprinting memory in mouse clone embryos produced from day 11.5 primordial germ cells. Development *129*, 1807–1817.

Mintz, B., and Russell, E.S. (1957). Gene-induced embryological modifications of primordial germ cells in the mouse. J. Exp. Zool. *134*, 207–237.

Nakagawa, M., Koyanagi, M., Tanabe, K., Takahashi, K., Ichisaka, T., Aoi, T., Okita, K., Mochiduki, Y., Takizawa, N., and Yamanaka, S. (2008). Generation of induced pluripotent stem cells without Myc from mouse and human fibroblasts. Nat. Biotechnol. *26*, 101–106.

Nakagawa, M., Takizawa, N., Narita, M., Ichisaka, T., and Yamanaka, S. (2010). Promotion of direct reprogramming by transformation-deficient Myc. Proc. Natl. Acad. Sci. USA *107*, 14152–14157.

Nayernia, K., Nolte, J., Michelmann, H.W., Lee, J.H., Rathsack, K., Drusenheimer, N., Dev, A., Wulf, G., Ehrmann, I.E., Elliott, D.J., et al. (2006). In vitro-differentiated embryonic stem cells give rise to male gametes that can generate offspring mice. Dev. Cell *11*, 125–132.

Nichols, J., and Smith, A. (2009). Naive and primed pluripotent states. Cell Stem Cell *4*, 487–492.

Nichols, J., Silva, J., Roode, M., and Smith, A. (2009). Suppression of Erk signalling promotes ground state pluripotency in the mouse embryo. Development *136*, 3215–3222.

Ogawa, T., Aréchaga, J.M., Avarbock, M.R., and Brinster, R.L. (1997). Transplantation of testis germinal cells into mouse seminiferous tubules. Int. J. Dev. Biol. *41*, 111–122.

Ohinata, Y., Payer, B., O'Carroll, D., Ancelin, K., Ono, Y., Sano, M., Barton, S.C., Obukhanych, T., Nussenzweig, M., Tarakhovsky, A., et al. (2005). Blimp1 is a critical determinant of the germ cell lineage in mice. Nature *436*, 207–213.

Ohinata, Y., Sano, M., Shigeta, M., Yamanaka, K., and Saitou, M. (2008). A comprehensive, non-invasive visualization of primordial germ cell development in mice by the Prdm1-mVenus and Dppa3-ECFP double transgenic reporter. Reproduction *136*, 503–514.

Ohinata, Y., Ohta, H., Shigeta, M., Yamanaka, K., Wakayama, T., and Saitou, M. (2009). A signaling principle for the specification of the germ cell lineage in mice. Cell *137*, 571–584.

Ohta, H., Yomogida, K., Yamada, S., Okabe, M., and Nishimune, Y. (2000). Real-time observation of transplanted 'green germ cells': proliferation and differentiation of stem cells. Dev. Growth Differ. *42*, 105–112.

Okita, K., Ichisaka, T., and Yamanaka, S. (2007). Generation of germline-competent induced pluripotent stem cells. Nature *448*, 313–317.

Okita, K., Nakagawa, M., Hyenjong, H., Ichisaka, T., and Yamanaka, S. (2008). Generation of mouse induced pluripotent stem cells without viral vectors. Science *322*, 949–953.

Payer, B., Chuva de Sousa Lopes, S.M., Barton, S.C., Lee, C., Saitou, M., and Surani, M.A. (2006). Generation of stella-GFP transgenic mice: a novel tool to study germ cell development. Genesis *44*, 75–83.

Rathjen, J., Lake, J.A., Bettess, M.D., Washington, J.M., Chapman, G., and Rathjen, P.D. (1999). Formation of a primitive ectoderm like cell population, EPL cells, from ES cells in response to biologically derived factors. J. Cell Sci. *112*, 601–612.

Saitou, M., and Yamaji, M. (2010). Germ cell specification in mice: signaling, transcription regulation, and epigenetic consequences. Reproduction *139*, 931–942.

Saitou, M., Barton, S.C., and Surani, M.A. (2002). A molecular programme for the specification of germ cell fate in mice. Nature *418*, 293–300.

Seki, Y., Hayashi, K., Itoh, K., Mizugaki, M., Saitou, M., and Matsui, Y. (2005). Extensive and orderly reprogramming of genome-wide chromatin modifications associated with specification and early development of germ cells in mice. Dev. Biol. *278*, 440–458.

Seki, Y., Yamaji, M., Yabuta, Y., Sano, M., Shigeta, M., Matsui, Y., Saga, Y., Tachibana, M., Shinkai, Y., and Saitou, M. (2007). Cellular dynamics associated with the genome-wide epigenetic reprogramming in migrating primordial germ cells in mice. Development *134*, 2627–2638.

Takahashi, K., and Yamanaka, S. (2006). Induction of pluripotent stem cells from mouse embryonic and adult fibroblast cultures by defined factors. Cell *126*, 663–676.

Tesar, P.J., Chenoweth, J.G., Brook, F.A., Davies, T.J., Evans, E.P., Mack, D.L., Gardner, R.L., and McKay, R.D. (2007). New cell lines from mouse epiblast share defining features with human embryonic stem cells. Nature *448*, 196–199.

Thomson, J.A., Itskovitz-Eldor, J., Shapiro, S.S., Waknitz, M.A., Swiergiel, J.J., Marshall, V.S., and Jones, J.M. (1998). Embryonic stem cell lines derived from human blastocysts. Science *282*, 1145–1147.

Vincent, S.D., Dunn, N.R., Sciammas, R., Shapiro-Shalef, M., Davis, M.M., Calame, K., Bikoff, E.K., and Robertson, E.J. (2005). The zinc finger transcriptional repressor Blimp1/Prdm1 is dispensable for early axis formation but is required for specification of primordial germ cells in the mouse. Development *132*, 1315–1325.

Yamaguchi, S., Kimura, H., Tada, M., Nakatsuji, N., and Tada, T. (2005). Nanog expression in mouse germ cell development. Gene Expr. Patterns *5*, 639–646.

Yamaji, M., Seki, Y., Kurimoto, K., Yabuta, Y., Yuasa, M., Shigeta, M., Yamanaka, K., Ohinata, Y., and Saitou, M. (2008). Critical function of Prdm14 for the establishment of the germ cell lineage in mice. Nat. Genet. *40*, 1016–1022.

Ying, Q.L., Wray, J., Nichols, J., Batlle-Morera, L., Doble, B., Woodgett, J., Cohen, P., and Smith, A. (2008). The ground state of embryonic stem cell self-renewal. Nature *453*, 519–523.